Solitary excitations in one-dimensional spin chains

Anton Wöllert*
Institut für Theoretische Physik, Georg-August-Universität Göttingen, 37077 Göttingen, Germany

Andreas Honecker
Institut für Theoretische Physik, Georg-August-Universität Göttingen, 37077 Göttingen, Germany and
Fakultät für Mathematik und Informatik, Georg-August-Universität Göttingen, 37073 Göttingen, Germany
(Received 22 February 2012; published 30 May 2012)

We study the real-time evolution of solitary excitations in one-dimensional quantum spin chains using exact diagonalization and the density-matrix renormalization group. The underlying question of this work is the correspondence between classical solitons and solitons in quantum mechanics. While classical solitons as eigensolutions of nonlinear wave equations are localized and have a sharp momentum, this is not possible in the corresponding quantum case due to the linearity of the Schrödinger equation or, seen in a more pictorial way, because of the uncertainty relation. For the case of the *XXZ* model it is shown that the real-time evolution of quantum wave packets accompanied by spreading is in qualitative accordance with that predicted by classical solitons.

DOI: 10.1103/PhysRevB.85.184433 PACS number(s): 75.10.Pq, 75.40.Mg, 47.35.Fg

I. INTRODUCTION

Solitons, first mentioned by John Scott Russel in 1844, are outstanding objects in the field of nonlinear physics.[1] Their description as solutions of nonlinear wave equations needs to take into account the full nonlinearity of the problem. Based on the numerical findings by Zabusky and Kruskal,[2] the inverse scattering transform[3] (IST) was the first major framework used to systematically research the solutions and spectra of integrable[4] classical nonlinear wave equations like the sine-Gordon equation or the nonlinear Schrödinger equation. These soliton solutions are usually characterized by a constant shape and velocity which is due to the cancellation of dispersion and nonlinearity.

The extension of the term "soliton" to the quantum regime is not straightforward. On the one hand there are technical problems in quantizing a classical nonlinear wave equation to a quantum field theory. For classical models amenable to the IST a direct canonical quantization is possible[5] because the IST can be seen as a nonlinear canonical mapping to action-angle variables which can be directly quantized. Quasiclassical quantization[6] has also been used for identifying classical with quantum systems. But still an obvious problem seems to exist in the quantum case. This is the interpretation of a quantum soliton, because a quantum soliton should not have a constant shape and velocity (due to the uncertainty relation) as is the case for a classical soliton. Another point of view on this problem is that classical solitons are eigensolutions of nonlinear wave equations. These eigensolutions are localized by means of some observable like density or magnetization in space even if the system is translationally invariant. In the quantum case this is not possible,[7] because the eigensolutions are completely delocalized. Still, the construction of localized wave packets, consisting of eigensolutions peaked around a specific momentum, is possible. These wave packets will spread due to the (in general) nonlinear dispersion relation. Notice that now, as opposed to the classical wave equation, there is no nonlinearity (the Schrödinger equation is linear) that could cancel the effect of dispersion. Thus in accordance with the uncertainty relation, the initial wave packet will spread. As is the case for the free particle in quantum mechanics, the transition to classical mechanics means that the spreading goes to zero.

Recent work[8–14] on the quantum dynamical aspects of solitons pursues the path of comparing mean-field approximations with the quantum model. The mean-field approach basically leads to a classical nonlinear equation of motion for some operator expectation value restricted to a subset of carefully chosen states (mainly product states). This classical nonlinear equation for an operator expectation value, e.g., $\langle \hat{a} \rangle$ for the condensate density in a Bose-Einstein condensate, might exhibit soliton solutions. Its time evolution is then compared for both the mean-field approximation as well for the quantum evolution on the full Hilbert space. One intrinsic problem of this approach is that it has to be justified that the mean-field approximation is still valid for the time evolution and not just for its initial state. We take a different route in that we identify directly a classical nonlinear model with a quantum model using direct canonical quantization. Therefore we will get a one-to-one correspondence between classical soliton solutions and their quantum mechanical counterparts, or vice versa. Thus, in our description, both the classical and the quantum models exhibit the same soliton solutions, and there is no intrinsic quantum soliton that does not exist in the classical theory or the other way round. In that sense we define the term "quantum soliton" as a state that corresponds up to the uncertainty relation to a classical soliton state. It is an interesting question if there exist models that exhibit intrinsic quantum solitons which do not occur in the corresponding classical theory. But before answering this question, a scheme for describing or defining an intrinsic quantum soliton must be found.

The simulation of real-time dynamics in quantum systems is a numerically hard problem due to the exponential increase of the Hilbert space with system size. The development of the density-matrix renormalization group[15,16] (DMRG) algorithm and its real-time variant the time-dependent DMRG (t-DMRG) (Refs. 16–18) has opened up new perspectives in simulating

one-dimensional (1D) systems, whose size is far beyond those that are reachable by exact diagonalization (ED) (see, for example, Refs. 8,14,19–21). Both methods allow us to create wave packets for larger systems.

In the following we will show that quantum wave packets can be constructed whose time evolution is in agreement (despite the quantum mechanical spreading) with their classical soliton counterparts.

II. THE MODEL

To investigate the correspondence between classical and quantum mechanical solitons, we use a 1D spin chain as our model. For the ferromagnetic easy-axis spin chain, as described in the following paragraphs, exact solutions for the energy spectra of the low-lying solutions exist. Both models are integrable, the classical in the sense of the inverse scattering transform[3] and the $s = \frac{1}{2}$ quantum model in the sense of the Bethe ansatz.[22] Furthermore, a clear mapping between the two models exists, and thus facilitates the comparison between classical and quantum eigensolutions and their spectra.

A. Quantum model

The quantum model is described by the anisotropic Heisenberg Hamiltonian

$$\hat{H} = -J \sum_i \left[\frac{1}{2} (\hat{S}_i^+ \hat{S}_{i+1}^- + \hat{S}_{i+1}^+ \hat{S}_i^-) + \Delta \hat{S}_i^z \hat{S}_{i+1}^z \right]. \quad (1)$$

We assume a ferromagnetic coupling $J > 0$ and easy-axis anisotropy $1 < \Delta = 1 + \Delta_z = \cosh \Phi$. Our reason for taking easy-axis anisotropy ($1 < \Delta$) is that in this case the analytical treatment of both the quantum and the classical models is simplest.[23,24] The ground state of this model is twofold degenerate (all spins pointing up or down). In the following we will take the state $|\downarrow\downarrow \ldots \downarrow\downarrow\rangle$ as the reference ground state. Note that the $s = \frac{1}{2}$ version of Eq. (1) is equivalent to a hard-core Bose-Hubbard model.[25] Consequently, each flipped spin with respect to the references state can be interpreted as occupation by one boson.

The energy for the lowest-lying excitations with momentum $-\pi \leqslant k \leqslant \pi$ and magnetization m (number of flipped spins) for $s = \frac{1}{2}$ is given by[23]

$$E_m(k) = J \left(\cosh m\Phi - \cos k\right) \frac{\sinh \Phi}{\sinh m\Phi} \quad (2)$$

in the thermodynamic limit. These excitations are also called m-magnon bound states and are completely delocalized over the whole system. To get localized excitations (i.e., where the magnetization is distributed over a region of a few sites), which could correspond to localized classical solitons, it is necessary to construct wave packets. These wave packets will consist of m-magnon bound states with different momenta. If this momentum distribution is peaked around k, we expect a group velocity given by the derivative of (2):

$$v_G(m,k) = J \sin k \frac{\sinh \Phi}{\sinh m\Phi}. \quad (3)$$

The maximum velocity of these wave packets is hence given by

$$v_{\max}(m) = v_G\left(m, \pm \frac{\pi}{2}\right) = \pm J \frac{\sinh \Phi}{\sinh m\Phi}. \quad (4)$$

B. Classical model

The classical model is described by the Landau-Lifshitz equation (LLE).[26] It can be derived from (1) by two approximations:

(1) $\hat{\boldsymbol{S}} \to \boldsymbol{S} = s\,(\sin\theta\cos\varphi, \sin\theta\sin\varphi, \cos\theta)^{\mathrm{t}}$, the classical treatment of spins which leads to an error of order $\frac{1}{s}$.

(2) $\boldsymbol{S}_i \to \boldsymbol{S}(x_i)$, the continuum treatment via the long-wavelength approximation with an error of order Δ_z^2 for low-lying excitations.

The classical Hamiltonian is then given by

$$H = J \int dx \left[\frac{1}{2} \left(\frac{\partial \boldsymbol{S}}{\partial x} \right)^2 + \Delta_z \left(s^2 - S_z^2 \right) \right]. \quad (5)$$

For the low-energy excitations of this Hamiltonian (one-soliton solutions), the quasiclassical quantization[27] gives an energy dispersion[6]

$$E(m,k) = 4s^2 J \sqrt{2\Delta_z} \left(\frac{\cosh m\sqrt{2\Delta_z}/2s - \cos k}{\sinh m\sqrt{2\Delta_z}/2s} \right). \quad (6)$$

It can be seen that for $s = \frac{1}{2}$ (6) is exactly the same as (2) to first order in Δ_z. Hence, even for the "most" quantumlike case ($s = \frac{1}{2}$), the energy spectra of the low-energy excitations are identical for both the quantum and the classical models. This leads naturally to an identification between classical and quantum solutions. But it is anyway an oddity that the classical spin profile $\boldsymbol{S}(x)$ is localized in space and the quantum profile $\langle \hat{S}_i \rangle$ is completely delocalized. So in order to get a classical profile coming from the quantum model, it seems natural to build wave packets as in the well-known problem of a free particle.

III. NUMERICAL INVESTIGATIONS

In the following simulations we assume $J = 1$ and $s = \frac{1}{2}$. The DMRG and t-DMRG algorithms were used for Figs. 1 and 5 using open boundary conditions and a discarded weight of 10^{-9} for the time evolutions.[28] Exact diagonalization for calculating the time evolution was used in Figs. 2, 3, and 4. Here, periodic boundary conditions were used in order to calculate the weights in Eq. (8) below in the basis of momentum eigenstates. For both methods a second-order Trotter decomposition[29] with $\Delta t = 0.01$ was used for time evolution.

A. Single spin flips

A very crude way to create wave packets is by flipping single spins from the ground state. This will lead to a very broad distribution in momentum space, meaning that excitations with different momenta and magnetization will be created. This can be seen clearly in Fig. 1. Three spins are flipped in the middle of the chain. The lines correspond to excitations with maximum group velocity $v_{\max}$ according to (4) for different m (= 3,2,1 from left to right) and Δ. Thus, it can be seen

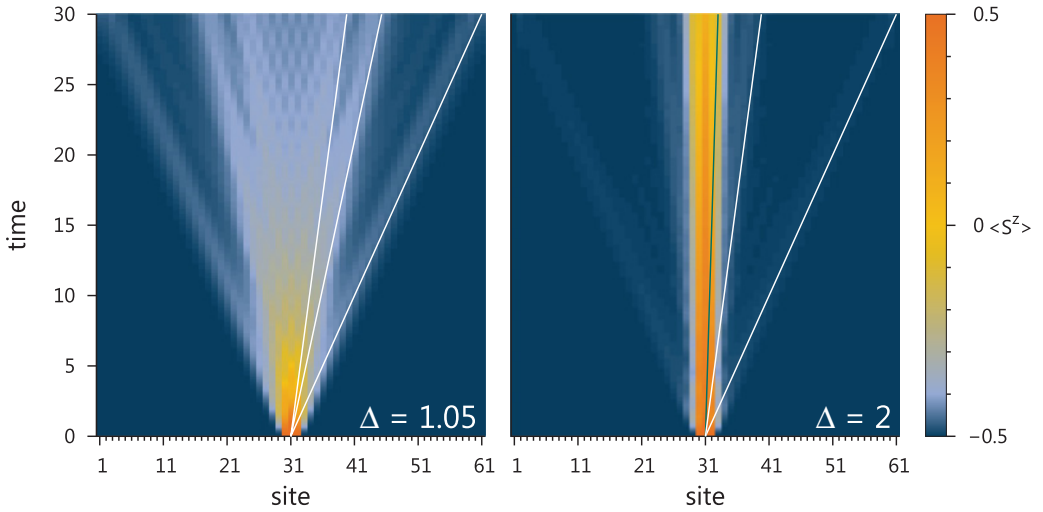

FIG. 1. (Color online) Time evolution of Fock state $|\downarrow\downarrow \ldots \downarrow\uparrow\uparrow\uparrow\downarrow \ldots \downarrow\downarrow\rangle$ for $s = \frac{1}{2}$ and $\Delta = 1.05$ (left) and $\Delta = 2$ (right). Lines show the expected movement with maximum group velocity $v_{\max}$ [see (4)].

that also one-magnon (spin waves) and two-magnon bound states are excited by a simple three-spin flip. This is consistent, because for $m = 3$ there exist higher excitations consisting of $m = 2$ bound states plus one $m = 1$ scattering state as well as $3 \times (m = 1)$ scattering states. From the point of view of classical integrability, meaning that excitations will go through each other without interaction, this dissection of the spectra is also necessary. If, for example, our initial state consists of $2 \times$ three-magnon wave packets, these will not disperse into $3 \times$ two-magnon wave packets during a collision because the time evolution will always stay in the initial $2 \times$ three-magnon bound-state sector.

B. Constructing wave packets

The following way to create specific excitations is based on the ideas of Ref. 30 to create dark solitons in Bose-Einstein condensates. Our scheme is very similar and consists of three main steps:

(1) Instead of flipping m spins in the middle of the chain, a more delocalized (in real space) wave packet will be created by adding a magnetic field B_{loc} to the Hamiltonian (1) which will attract the flipped spins to the middle. Thus, numerical methods will yield a ground state where the flipped spins (whose number can be set by the initial magnetization) rest at the center.

(2) Because of the symmetry, in momentum space the wave packet will be localized around $k = 0$. In order to kick this wave packet an additional time evolution is done just with a specific magnetic field B_{phase}.

(3) After this initial preparation of the wave packet, its free time evolution under the Hamiltonian (1) can be investigated.

Previous numerical work using this method has been done in Refs. 8–10.

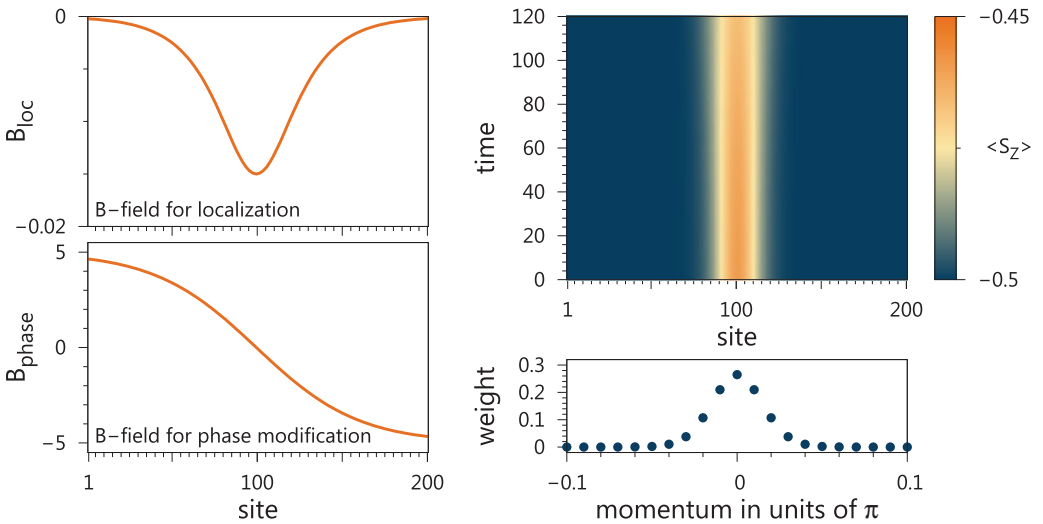

FIG. 2. (Color online) Left: Schematic profile of the magnetic fields for localizing the excitation and for shifting its momentum distribution. Right: Time evolution of a localized excitation ($m = 1$, $\Delta = 1.05$) and its momentum distribution before application of $\hat{H}_{\text{phase}}$. Its initial width is bigger than in Fig. 1 but it spreads only slightly because of the sharp momentum distribution around $k = 0$.

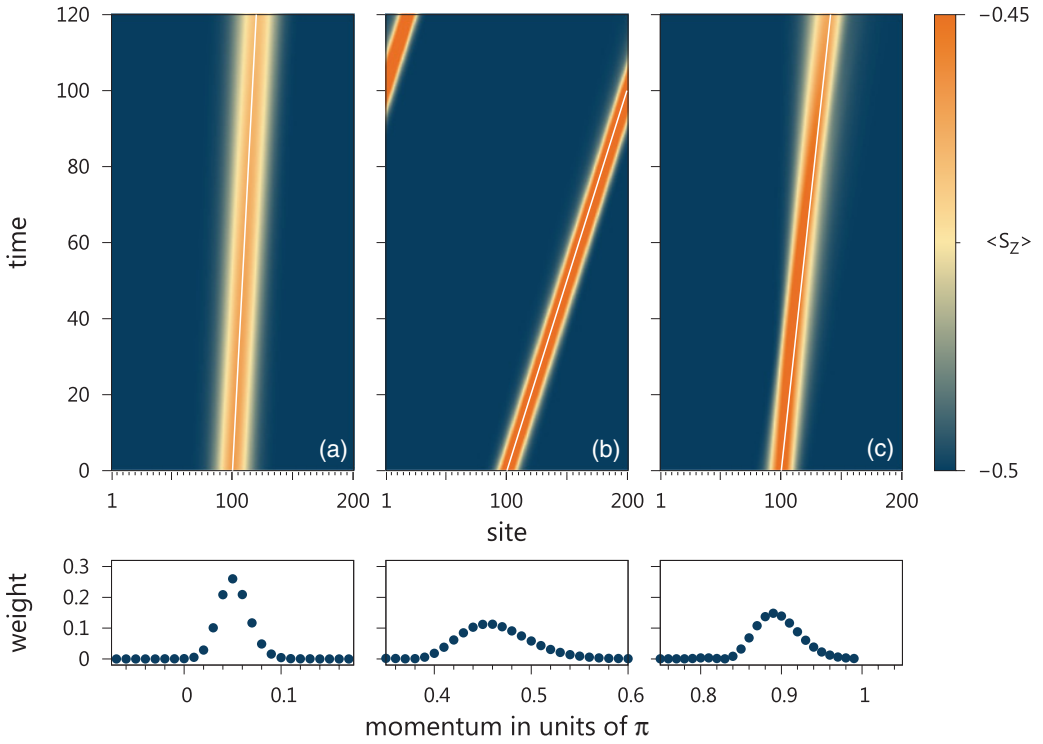

FIG. 3. (Color online) Time evolution for $m = 1$, $\Delta = 1.05$ using different $\hat{H}_{\rm loc}$ and $\hat{H}_{\rm phase}$ (see Table I) and its momentum distribution. White lines show the expected movement with group velocity $v_g(k_P)$, where k_P is the momentum with maximum weight.

1. Localizing the wave packet

Because a simple spin flip creates a completely localized excitation, the momentum distribution will be completely smeared out and the localized excitation will dislocate very quickly. To get an initial state which is also localized in momentum space it is thus necessary to have some delocalization in real space. To create such a state, we add a magnetic field for localization (see Fig. 2) to the Hamiltonian (1) of the following form:

$$\hat{H}_{\rm loc} = \sum_i \frac{1}{s} B_{\rm loc}[i] \cdot \hat{S}_i^z$$

$$\text{with} \quad B_{\rm loc}[i] = -\frac{B_{\rm locA}}{\cosh\left(\frac{x_0 - i}{B_{\rm locW}}\right)}. \tag{7}$$

Fixing the magnetization m (i.e., the number of flipped spins) and calculating the ground state will result in a magnetization profile as can be seen in the right part of Fig. 2. The term $\hat{H}_{\rm loc}$ is used only for the initial state. Time evolution is done just with (1). The parameters $B_{\rm locA}$ and $B_{\rm locW}$ control the depth and width of the magnetic field and therefore the localization of the wave packet.

Using exact diagonalization in momentum space, the projection of the initial state onto the momentum eigenstates of (1) can be calculated as well as their weight:

$$\text{weight}\,(k,\alpha) = |\langle \psi_{\rm excited} | k_\alpha \rangle|. \tag{8}$$

The index α runs through the number of eigenstates with momentum k. For $m = 1$, there is just one such eigenstate for each k. This weight distribution is shown below the time evolutions in Figs. 2 and 3. The peaked momentum distribution around $k = 0$ in Fig. 2 clarifies the stability of the magnetization profile.

2. Kicking the wave packet

To get the localized wave packet into movement it is necessary to shift the momentum distribution to a $k \neq 0$. Changing the phase of each Fock state in real space that the initial state consists of will not change the magnetization profile but the momentum distribution. This phase change can be implemented by a time evolution of the initial state with the following Hamiltonian:

$$\hat{H}_{\rm phase} = \sum_i \frac{1}{s} B_{\rm phase}[i] \hat{S}_i^z$$

$$\text{with} \quad B_{\rm phase}[i] = B_{\rm phA} \tanh\left(\frac{x_0 - i}{B_{\rm phW}}\right). \tag{9}$$

The magnetic field $B_{\rm phase}[i]$ (sketched in Fig. 2) would also suggest that the wave packet would slide down to the right corresponding to a momentum shift to $k > 0$. This is indeed the case as can be seen in Fig. 3. $B_{\rm phA}$ and $B_{\rm phW}$ modify the

TABLE I. Parameters for $\hat{H}_{\rm loc}$ and $\hat{H}_{\rm phase}$ to generate the excitations shown in Figs. 3 and 4.

Case	$B_{\rm locA}$	$B_{\rm locW}$	$B_{\rm phA}$	$B_{\rm phW}$
(a)	0.0075	20	5	60
(b)	0.02	7	22.5	30
(c)	0.15	50	85.5	60
(d)	0.05	10	15	40

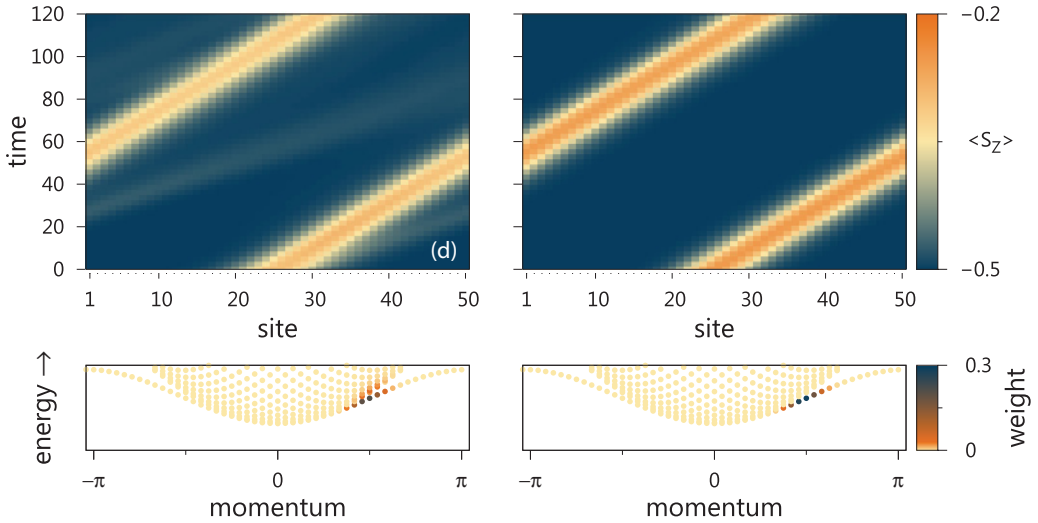

FIG. 4. (Color online) Left: Time evolution for $m = 2$, $\Delta = 1.05$ using $\hat{H}_{\rm loc}$ and $\hat{H}_{\rm phase}$ as specified for case (d) in Table I. A faster ray to the right of the main $m = 2$ moving bound excitation can be seen, which is attributed to the weight in the $m = 1 + 1$ scattering sector of the momentum distribution. Right: By projecting out the states with the weight in the $m = 1 + 1$ scattering sector, the faster ray disappears.

amplitude and width of the phase-imprinting magnetic field. Concerning the length $t_{\rm phase}$ of the time evolution with $\hat{H}_{\rm phase}$ it should be noted that the phase-imprinted state depends only on the product $t_{\rm phase} B_{\rm phA}$. That is why we fixed $t_{\rm phase} = 1$ and varied $B_{\rm phA}$. Figure 3 shows thus that the picture of moving wave packets with specific group velocity (defined by the peak in their momentum distribution) is consistent. The parameters for $\hat{H}_{\rm loc}$ and $\hat{H}_{\rm phase}$ were found[31] by trial and error and are given in Table I.

Use of this scheme for creating wave packets with $m > 1$ will of course result also in other higher excitations. This is shown in Fig. 4 for $m = 2$. The slower-moving excitation in the left part corresponds to a two-bound wave packet, while the faster light one corresponds to a spin wave. The distribution in momentum space also shows this. By using exact diagonalization in momentum space it is possible to project out these spin wave excitations from the $2 \times (m = 1)$ sector of the excitation spectra. The result of this projection (the disappearance of the faster spin-wave excitation) is seen in the right part of Fig. 4.

3. *Colliding wave packets*

Using the methods described before it is also possible to create two wave packets on a chain.[32] Various scenarios can

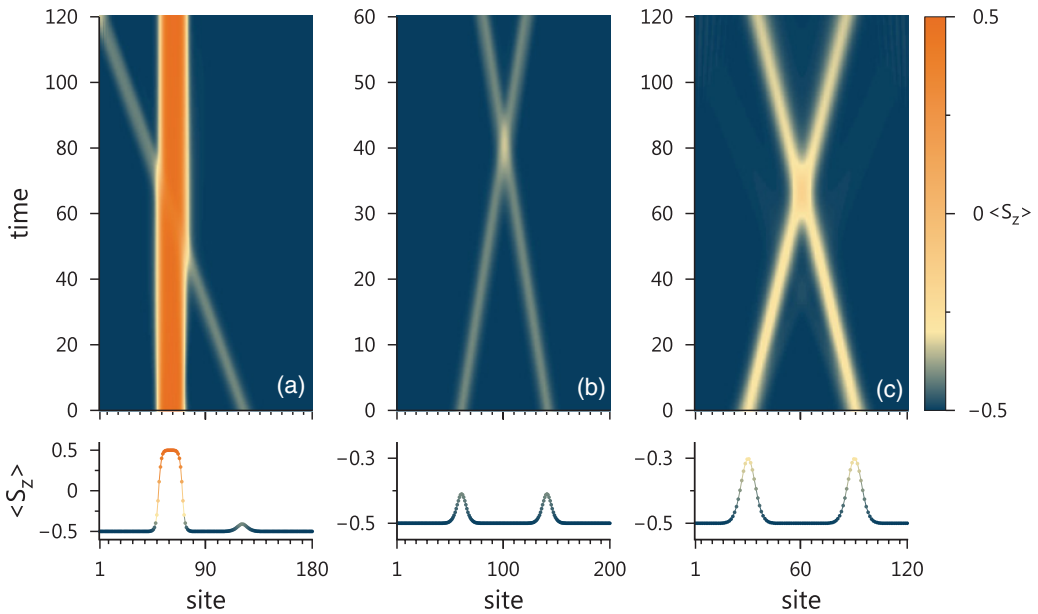

FIG. 5. (Color online) Top: Time evolution of different combined excitations ($\Delta = 1.05$; for other parameters see Table II). (a) Spin-wave packet ($m = 1$) running through a large static magnon complex consisting of two bound domain walls ($m = 20$) and shifting it by one site to the right. (b) Two spin-wave packets ($m = 1$) running through each other. (c) Two magnon packets ($m = 2$) running through each other. Bottom: Corresponding initial magnetization profile.

TABLE II. Parameters for $\hat{H}_{\mathrm{loc}}$ and $\hat{H}_{\mathrm{phase}}$ to generate the excitations shown in Fig. 5.

Case		B_{locA}	B_{locW}	B_{phA}	B_{phW}
(a)	Left: $N_M = 20, x_0 = 60$	0.05	5	0	25
	Right: $N_M = 1, x_0 = 120$	0.02	5	-20	25
(b)	Left: $N_M = 1, x_0 = 30$	0.02	5	20	25
	Right: $N_M = 1, x_0 = 70$	0.02	5	-20	25
(c)	Left: $N_M = 2, x_0 = 30$	0.05	10	15	40
	Right: $N_M = 2, x_0 = 90$	0.05	10	-15	40

be obtained this way. Figure 5 shows three types of collision. The first (a) shows the passing of an $m = 1$ spin wave through a resting $m = 20$ bound state (which can be considered as two bound domain walls). The movement of the domain wall by exactly one site (corresponding to one unit of magnetization $m = 1$) was predicted earlier in Ref. 33 and can be seen here. The other two settings (b) and (c) show the collision of two $m = 1$ and $m = 2$ wave packets, propagating in opposite directions. As known from classical integrability, these excitations should just go through each other, because their characteristics (i.e., momentum and magnetization) represent integrals of motion. The parameters used for these calculations are given in Table II.

IV. CONCLUSION

Based on the analytical findings of Ref. 24, we investigated the real-time evolution of quantum wave packets in the ferromagnetic easy-axis Heisenberg model. They were constructed in a way close to their classical soliton counterparts by using additional magnetic fields to localize them and to give them a momentum kick. The time evolution is consistent with the classical picture of the integrable LLE and in the case of the setting shown in Fig. 5(a) explicitly shows the analytical predictions of Ref. 33.

This method of constructing localized wave packets might also be used for nonintegrable quantum systems, where colliding wave packets might excite each other or slow down and create new excitations from the background. Furthermore, it might be used for examining transport properties in spin systems.

ACKNOWLEDGMENTS

We thank H. J. Mikeska and A. K. Kolezhuk for useful discussions. A.W. would like to thank R. Peters and P. E. Dargel for support on the DMRG code. Parts of the DMRG code were based on prior work by R. Peters. A.H. acknowledges support by the Deutsche Forschungsgemeinschaft via a Heisenberg Fellowship (Project No. HO 2325/4-2).

*anton.woellert@mpi-hd.mpg.de

[1] A. C. Scott, F. Y. F. Chu, and D. W. McLaughlin, Proc. IEEE **61**, 1443 (1973).
[2] N. J. Zabusky and M. D. Kruskal, Phys. Rev. Lett. **15**, 240 (1965).
[3] C. S. Gardner, J. M. Greene, M. D. Kruskal, and R. M. Miura, Phys. Rev. Lett. **19**, 1095 (1967).
[4] The term "integrable" is well defined for classical mechanics. As for quantum mechanics, we use this term in the sense of "soluble by the quantum inverse scattering method" (see Ref. 34).
[5] V. E. Zakharov and L. D. Faddeev, Funct. Anal. Appl. **5**, 280 (1971).
[6] A. M. Kosevich, B. A. Ivanov, and A. S. Kovalev, Fiz. Nizk. Temp. **3**, 906 (1977) [Sov. J. Low. Temp. Phys. **3**, 440 (1977)].
[7] Localized eigenstates for translationally invariant quantum models might exist if the model has a flat band [as for quite a few frustrated models (Refs. 35, 36)], but for the quantized versions of the nonlinear wave equations mentioned in this work, this is not the case. Furthermore, these types of localized eigenstate cannot move because the group velocity in a flat band is zero.
[8] R. V. Mishmash, I. Danshita, C. W. Clark, and L. D. Carr, Phys. Rev. A **80**, 053612 (2009).
[9] R. V. Mishmash and L. D. Carr, Phys. Rev. Lett. **103**, 140403 (2009).
[10] R. V. Mishmash and L. D. Carr, Math. Comput. Simul. **80**, 732 (2009).
[11] R. Balakrishnan, I. I. Satija, and C. W. Clark, Phys. Rev. Lett. **103**, 230403 (2009).
[12] I. I. Satija and R. Balakrishnan, Phys. Lett. A **375**, 517 (2011).
[13] W. P. Reinhardt, I. I. Satija, B. Robbins, and C. W. Clark, arXiv:1102.4042.
[14] C. P. Rubbo, I. I. Satija, W. P. Reinhardt, R. Balakrishnan, A. M. Rey, and S. R. Manmana, Phys. Rev. A **85**, 053617 (2012).
[15] S. R. White, Phys. Rev. Lett. **69**, 2863 (1992).
[16] U. Schollwöck, Ann. Phys. (NY) **326**, 96 (2011).
[17] G. Vidal, Phys. Rev. Lett. **91**, 147902 (2003).
[18] A. J. Daley, C. Kollath, U. Schollwöck, and G. Vidal, J. Stat. Mech. Theory Exp. (2004) P04005.
[19] D. Gobert, C. Kollath, U. Schollwöck, and G. Schütz, Phys. Rev. E **71**, 036102 (2005).
[20] S. R. Manmana, S. Wessel, R. M. Noack, and A. Muramatsu, Phys. Rev. B **79**, 155104 (2009).
[21] F. Heidrich-Meisner, S. R. Manmana, M. Rigol, A. Muramatsu, A. E. Feiguin, and E. Dagotto, Phys. Rev. A **80**, 041603 (2009).
[22] H. Bethe, Z. Phys. **71**, 205 (1931).
[23] A. A. Ovchinnikov, Pis'ma Zh. Eksp. Teor. Fiz. **5**, 48 (1967) [JETP Lett. **5**, 38 (1967)].
[24] A. M. Kosevich, B. A. Ivanov, and A. S. Kovalev, Phys. Rep. **194**, 117 (1990).
[25] T. Matsubara and H. Matsuda, Prog. Theor. Phys. **16**, 569 (1956).
[26] L. D. Landau and E. Lifschitz, Phys. Z. Sojwetunion **8**, 153 (1935).
[27] That is, identifying classical magnetization and momentum with their quantum mechanical counterparts.
[28] It should be noted that the time evolution in Figs. 1, 5(b), and 5(c) could have also been done using ED instead of the t-DMRG.
[29] M. Suzuki, Commun. Math. Phys. **51**, 183 (1976).
[30] L. D. Carr, J. Brand, S. Burger, and A. Sanpera, Phys. Rev. A **63**, 051601 (2001).

[31]It should be mentioned that these wave packets can be created directly by a superposition of the specific momentum eigenstates, if these are known analytically.

[32]In order to create more than one localized wave packet, it is necessary to remove the interactions (spin hopping) between the parts of the chain where these excitations should be placed. Otherwise all the magnetization will fall into one of the valleys of the magnetic field potential in the ground state.

[33]A. V. Mikhaĭlov and A. I. Yaremchuk, Pis'ma Zh. Eksp. Teor. Fiz. **39**, 296 (1984) [JETP Lett. **39**, 354 (1984)].

[34]V. E. Korepin, N. M. Bogoliubov, and A. G. Izergin, *Quantum Inverse Scattering Method and Correlation Functions* (Cambridge University Press, Cambridge, 1997).

[35]O. Derzhko, J. Richter, A. Honecker, and H.-J. Schmidt, Low Temp. Phys. **33**, 745 (2007).

[36]S. D. Huber and E. Altman, Phys. Rev. B **82**, 184502 (2010).